Principles of Guidance-Based Path Following in 2D and 3D

Morten Breivik*,[1]
*Centre for Ships and Ocean Structures (CESOS)
Norwegian University of Science and Technology (NTNU)
NO-7491 Trondheim, Norway
E-mail: morten.breivik@ieee.org

Thor I. Fossen*,†
†Department of Engineering Cybernetics (ITK)
Norwegian University of Science and Technology (NTNU)
NO-7491 Trondheim, Norway
E-mail: fossen@ieee.org

***Abstract*— This paper treats the subject of fundamental guidance principles related to motion behaviour in a 2D plane and a 3D space. In this context, the concept of guidance-based path following is defined and elaborated upon. Its specifics are contrasted towards the already established concept of trajectory tracking. Specifically, guidance laws are developed at an ideal, dynamics-independent level to yield generally valid laws uninfluenced by the particularities of any specific dynamics case. These laws can subsequently be tailored to actual target systems like e.g. watercraft or spacecraft, for instance in a cascaded setting. The approach renders all regular paths feasible. Possible applications and extensions to the guidance-based path following scheme are also briefly suggested.**

I. Introduction

The ability to maneuver an actual target system like a watercraft or a spacecraft accurately along a desired geometric path is a primary objective for most applications. An objective like satisfying some desired dynamic behaviour while traversing the path would consequently be viewed upon as secondary. If given the freedom to construct a desired geometric path for an actual system to converge to and follow, the choice of a solution strategy to fulfill the task at hand would traditionally stand between the concepts of trajectory tracking (TT) and path following (PF).

To illustrate the difference between these two schemes, we will employ the notion of an *actual particle* and a *path particle*. An actual particle is a position variable belonging to an actual system. It represents the position variable whose goal is to converge to and follow the desired geometric path. A path particle, on the other hand, is a position variable belonging to the desired geometric path, restricted to move along it at all times.

The TT scheme entails the simultaneous construction of the geometric path and the dynamic behaviour of the path particle. Hence, it inherently mixes the space and time assignments into one single assignment, demanding that any actual target system is located at a specific point in space at a specific, pre-assigned instant in time. Since the dynamic assignment is usually based on some a priori assumptions of the actual system capabilities to ensure its feasibility, it must be manually reparametrized if something should occur that would render the actual system incapable of satisfying it. And if no such tedious reparametrization is performed, the path particle is essentially left to propagate on its own, rendering the path system oblivious to the status of the actual system. As such, the TT scheme represents a feedforward, open loop type of solution at the path system-actual system interaction level.

The PF strategy, on the other hand, involves the separate construction of the geometric path and the dynamic assignment; emphasizing spatial localization as a primary task objective, while considering the dynamic aspect to be of secondary importance, sacrificable if necessary. This clearly represents a more flexible and robust alternative than the TT scheme. Specifically, this paper treats a PF concept where the dynamic assignment is associated with the actual particle, and where the path particle is designed to evolve according to the actual particle. Thus, the path particle can never leave the actual particle behind. This entails a closed loop type of solution to the problem at hand, with the path system adjusting itself to the actual system. This type of scheme requires that guidance laws are applied to guide the actual particle towards the geometric path, stemming from the fact that the path system now lacks a self-propelled attractor as in TT. Consequently, the term *guidance-based path following* is chosen to describe the concept. The guidance laws should also ensure that the convergence behaviour of the actual particle towards the path becomes elegant and natural, which is usually not the case when applying a traditional TT scheme. This is especially relevant for mechanical vehicle systems.

A. Previous Work

Pioneering work on the type of path following scheme under consideration can be found in a paper by Claude Samson [1], where the author considers path following for wheeled mobile robots. Omitting a dynamic model, the treatment is of a purely kinematic nature, making it comparable to the results of this paper. However, due to Samson's choice of the path particle as the exact projection of the actual

[1]This work was supported by the Research Council of Norway through the Centre for Ships and Ocean Structures at NTNU.

particle onto the desired geometric path, the results in [1] are only local. Also, Barbalat's lemma has to be applied in the stability analysis due to the way in which the guidance laws are chosen, entailing that only a convergence result can be concluded. However, the paper has served as an invaluable reference and guideline for most of the following work on the subject.

The initial inspiration for the work reported here can be traced back to three papers; namely those of Rysdyk [2], Pettersen and Lefeber [3], and Lapierre et al. [4]. They all essentially treat the problem of guidance-based path following, although the approaches could seem somewhat different at first sight. All consider the control of specific actual systems with distinctive dynamics, and as such intermix the core concepts of the guidance-based path following scheme with the control design. While [2] treats unmanned aerial vehicles (UAVs), [3] treats marine surface vessels (MSVs), and [4] treats autonomous underwater vehicles (AUVs). Relevant applications can also be found in Do and Pan [5], Encarnação and Pascoal [6], and del Río et al. [7].

B. Main Contribution

The main contribution of this paper is to develop a theoretical framework for the concept of guidance-based path following, which renders all regularly parametrized paths feasible. By extracting and extending the core concepts of application-specific cases, the essence is lifted out of any particular dynamic setting and onto an ideal level, to be able to state and analyse it properly. Hence, the resulting theory becomes generally valid. For the sake of intuition and page limitation, the paper only considers the planar 2D case and the spatial 3D case. The concept is nevertheless readily extendable to n-dimensional systems, and will be followed up with a more in-depth consideration in a separate publication.

II. Problem Statement

The primary objective in guidance-based path following is to ensure that the actual particle converges to and follows the desired geometric path, without any temporal requirements. The secondary objective is to ensure that the actual particle complies with a desired dynamic behaviour. By then using the convenient task classification scheme of Skjetne [8], the guidance-based path following problem can be expressed by the following two task objectives:

Geometric Task: Make the position of the actual particle converge to and follow a desired geometric path.

Dynamic Task: Make the speed of the actual particle converge to and track a desired speed assignment.

The geometric task implies that the actual particle must move at non-zero speed towards the path particle associated with the desired geometric path, and that the path particle in some sense also must move towards the actual particle despite being restricted to its path. The dynamic task then states that the dynamic (speed) assignment is associated with the actual particle, inherently implying that its motion must be guided by guidance laws if the geometric task is to be fulfilled. Also, note that when both task objectives for some reason cannot be met simultaneously, the geometric one should have precedence over the dynamic one.

III. Principles of Guidance in 2D and 3D

Here, the guidance laws required for solving the guidance-based path following problem are developed. We will consistently employ the notion of an *ideal particle*, which is to be interpreted as an actual particle without dynamics (i.e. it can instantly attain any assigned motion behaviour) free to move anywhere. By disregarding the dynamics, the guidance laws can be developed and stated in their purest form. This makes the theory as general as possible, which enables an extension to any desirable dynamics case at a later stage.

A. Assumptions

The following assumptions are made throughout the paper:

- **A.1** The desired geometric path is regularly parametrized.
- **A.2** The speed of the ideal particle is lower-bounded. Note that it is non-negative by definition.
- **A.3** The guidance variables are positive and upper-bounded, i.e. $\triangle_{\mathrm{i}}(t) \in \langle 0, \triangle_{\mathrm{i,max}}] \; \forall t \geq 0, \, i \in \mathcal{I}$, where $\mathcal{I}$ is an index set with appropriate dimension.

B. Principles of Guidance in 2D

This section develops the guidance laws required to solve the planar 2D case of the guidance-based path following problem.

Denote the inertial position and velocity vectors of the ideal particle by $\mathbf{p} = [x, y]^\top \in \mathbb{R}^2$ and $\dot{\mathbf{p}} = [\dot{x}, \dot{y}]^\top \in \mathbb{R}^2$, respectively. The velocity vector has two characteristics; size and orientation. Denote the size by $U = |\dot{\mathbf{p}}|_2 = (\dot{\mathbf{p}}^\top \dot{\mathbf{p}})^{\frac{1}{2}}$ (the speed), and let the orientation be characterized by the angular variable:

$$\chi = \arctan\left(\frac{\dot{y}}{\dot{x}}\right), \tag{1}$$

which is denoted the azimuth angle. These are the variables that must be manipulated in order to solve the problem at hand as far as the ideal particle is concerned. Since it is assumed that both U and χ can attain any desirable value instantaneously, rewrite them as U_{d} and χ_{d}.

Then consider a geometric path continuously parametrized by a scalar variable $\varpi \in \mathbb{R}$, and denote the position of its path particle as $\mathbf{p}_{\mathrm{p}}(\varpi) \in \mathbb{R}^2$. Consequently, the geometric path can be expressed by the set:

$$\mathcal{P} = \left\{ \mathbf{p} \in \mathbb{R}^2 \mid \mathbf{p} = \mathbf{p}_{\mathrm{p}}(\varpi) \; \forall \varpi \in \mathbb{R} \right\}, \tag{2}$$

where $\mathcal{P} \subset \mathbb{R}^2$.

For a given ϖ, define a local reference frame at $\mathbf{p}_{\mathrm{p}}(\varpi)$ and name it the PATH frame (**P**). To arrive at **P**, we need to positively rotate the INERTIAL frame (**I**) an angle:

$$\chi_{\mathrm{p}}(\varpi) = \arctan\left(\frac{y'_{\mathrm{p}}(\varpi)}{x'_{\mathrm{p}}(\varpi)}\right) \tag{3}$$

about its z-axis, where the notation $x'_{\mathrm{p}}(\varpi) = \frac{\mathrm{d}x_{\mathrm{p}}}{\mathrm{d}\varpi}(\varpi)$ has been utilized. This rotation can be represented by the rotation matrix:

$$\mathbf{R}_{\mathrm{p,z}}(\chi_{\mathrm{p}}) = \begin{bmatrix} \cos\chi_{\mathrm{p}} & -\sin\chi_{\mathrm{p}} \\ \sin\chi_{\mathrm{p}} & \cos\chi_{\mathrm{p}} \end{bmatrix}, \tag{4}$$

where $\mathbf{R}_{\mathrm{p,z}} \in SO(2)$. Consequently, the error vector between $\mathbf{p}$ and $\mathbf{p}_{\mathrm{p}}(\varpi)$ expressed in $\mathbf{P}$ is given by:

$$\boldsymbol{\varepsilon} = \mathbf{R}_{\mathrm{p}}^{\top}(\mathbf{p} - \mathbf{p}_{\mathrm{p}}(\varpi)), \tag{5}$$

where $\boldsymbol{\varepsilon} = [s, e]^{\top} \in \mathbb{R}^2$ consists of the *along-track error* s and the *cross-track error* e; see Figure 1. The along-track error represents the (longitudinal) distance from $\mathbf{p}_{\mathrm{p}}(\varpi)$ to $\mathbf{p}$ along the x-axis of the PATH frame, while the cross-track error represents the (lateral) distance along the y-axis. Also, recognize the notion of the *off-track error* $|\boldsymbol{\varepsilon}|_2 = \sqrt{s^2 + e^2}$. It is clear that the geometric task is solved by driving the off-track error to zero.

Consequently, by differentiating $\boldsymbol{\varepsilon}$ with respect to time, we obtain:

$$\dot{\boldsymbol{\varepsilon}} = \dot{\mathbf{R}}_{\mathrm{p}}^{\top}(\mathbf{p} - \mathbf{p}_{\mathrm{p}}) + \mathbf{R}_{\mathrm{p}}^{\top}(\dot{\mathbf{p}} - \dot{\mathbf{p}}_{\mathrm{p}}), \tag{6}$$

where:

$$\dot{\mathbf{R}}_{\mathrm{p}} = \mathbf{R}_{\mathrm{p}}\mathbf{S}_{\mathrm{p}} \tag{7}$$

with:

$$\mathbf{S}_{\mathrm{p}} = \begin{bmatrix} 0 & -\dot{\chi}_{\mathrm{p}} \\ \dot{\chi}_{\mathrm{p}} & 0 \end{bmatrix}, \tag{8}$$

which is skew-symmetric; $\mathbf{S}_{\mathrm{p}} = -\mathbf{S}_{\mathrm{p}}^{\top}$. We also have that:

$$\dot{\mathbf{p}} = \dot{\mathbf{p}}_{\mathrm{dv}} = \mathbf{R}_{\mathrm{dv}}\mathbf{v}_{\mathrm{dv}}, \tag{9}$$

where:

$$\mathbf{R}_{\mathrm{dv}} = \mathbf{R}_{\mathrm{dv,z}}(\chi_{\mathrm{d}}) \tag{10}$$

$$= \begin{bmatrix} \cos\chi_{\mathrm{d}} & -\sin\chi_{\mathrm{d}} \\ \sin\chi_{\mathrm{d}} & \cos\chi_{\mathrm{d}} \end{bmatrix} \tag{11}$$

with $\mathbf{R}_{\mathrm{dv}} \in SO(2)$. This matrix represents a rotation from the INERTIAL frame to a frame attached to the ideal particle with its x-axis along the velocity vector of the particle. Let this frame be called the DESIRED VELOCITY frame (**DV**). Hence, the vector $\mathbf{v}_{\mathrm{dv}} = [U_{\mathrm{d}}, 0]^{\top} \in \mathbb{R}^2$ represents the ideal particle velocity with respect to **I**, represented in **DV**. Additionally, we have that:

$$\dot{\mathbf{p}}_{\mathrm{p}} = \mathbf{R}_{\mathrm{p}}\mathbf{v}_{\mathrm{p}}, \tag{12}$$

where $\mathbf{v}_{\mathrm{p}} = [U_{\mathrm{p}}, 0]^{\top} \in \mathbb{R}^2$ represents the path particle velocity with respect to **I**, represented in **P**.

By then expanding (6) in light of the recent discussion, we get:

$$\begin{aligned} \dot{\boldsymbol{\varepsilon}} &= (\mathbf{R}_{\mathrm{p}}\mathbf{S}_{\mathrm{p}})^{\top}(\mathbf{p} - \mathbf{p}_{\mathrm{p}}) + \mathbf{R}_{\mathrm{p}}^{\top}(\mathbf{R}_{\mathrm{dv}}\mathbf{v}_{\mathrm{dv}} - \mathbf{R}_{\mathrm{p}}\mathbf{v}_{\mathrm{p}}) \\ &= \mathbf{S}_{\mathrm{p}}^{\top}\boldsymbol{\varepsilon} + \mathbf{R}_{\mathrm{p}}^{\top}\mathbf{R}_{\mathrm{dv}}\mathbf{v}_{\mathrm{dv}} - \mathbf{v}_{\mathrm{p}}. \end{aligned} \tag{13}$$

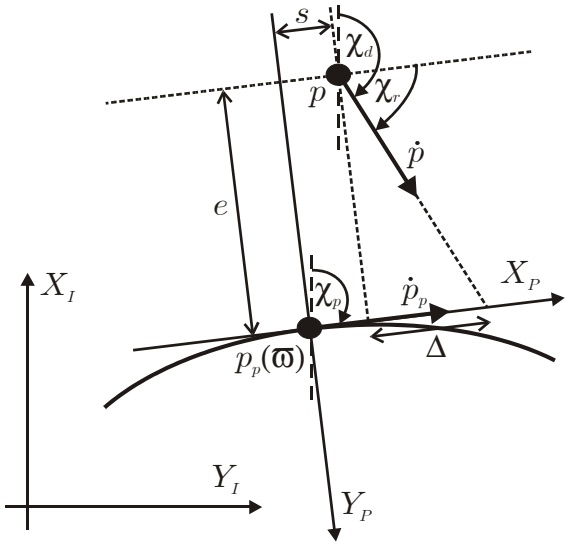

Fig. 1. The geometric principle of the proposed guidance-based path following scheme in 2D.

Now define the positive definite and radially unbounded Control Lyapunov Function (CLF):

$$V_{\boldsymbol{\varepsilon}} = \frac{1}{2}\boldsymbol{\varepsilon}^{\top}\boldsymbol{\varepsilon} = \frac{1}{2}(s^2 + e^2), \tag{14}$$

and differentiate it with respect to time along the trajectories of $\boldsymbol{\varepsilon}$ to obtain:

$$\begin{aligned} \dot{V}_{\boldsymbol{\varepsilon}} &= \boldsymbol{\varepsilon}^{\top}\dot{\boldsymbol{\varepsilon}} \\ &= \boldsymbol{\varepsilon}^{\top}\left(\mathbf{S}_{\mathrm{p}}^{\top}\boldsymbol{\varepsilon} + \mathbf{R}_{\mathrm{p}}^{\top}\mathbf{R}_{\mathrm{dv}}\mathbf{v}_{\mathrm{dv}} - \mathbf{v}_{\mathrm{p}}\right) \\ &= \boldsymbol{\varepsilon}^{\top}\left(\mathbf{R}_{\mathrm{p}}^{\top}\mathbf{R}_{\mathrm{dv}}\mathbf{v}_{\mathrm{dv}} - \mathbf{v}_{\mathrm{p}}\right) \end{aligned} \tag{15}$$

since the skew-symmetry of $\mathbf{S}_{\mathrm{p}}$ leads to $\boldsymbol{\varepsilon}^{\top}\mathbf{S}_{\mathrm{p}}^{\top}\boldsymbol{\varepsilon} = 0$. By further expansion, we get:

$$\dot{V}_{\boldsymbol{\varepsilon}} = s(U_{\mathrm{d}}\cos(\chi_{\mathrm{d}} - \chi_{\mathrm{p}}) - U_{\mathrm{p}}) + eU_{\mathrm{d}}\sin(\chi_{\mathrm{d}} - \chi_{\mathrm{p}}). \tag{16}$$

At this point, it seems natural to consider the path particle speed U_{p} as a virtual input for stabilizing s. Consequently, by choosing U_{p} as:

$$U_{\mathrm{p}} = U_{\mathrm{d}}\cos(\chi_{\mathrm{d}} - \chi_{\mathrm{p}}) + \gamma s, \tag{17}$$

where $\gamma > 0$ becomes a constant gain parameter in the guidance law, we achieve:

$$\dot{V}_{\boldsymbol{\varepsilon}} = -\gamma s^2 + eU_{\mathrm{d}}\sin(\chi_{\mathrm{d}} - \chi_{\mathrm{p}}), \tag{18}$$

which shows that the task of the path particle is to ensure that the along-track error s converges to zero. This means that the path particle will continuously track the ideal particle.

What remains is thus to ensure that the cross-track error e also converges to zero. This is the responsibility of the ideal particle, and beyond anything that the path particle can achieve. Equation (18) shows that $(\chi_{\mathrm{d}} - \chi_{\mathrm{p}})$ can be considered a virtual input for stabilizing e. Denote this angular difference by $\chi_{\mathrm{r}} = \chi_{\mathrm{d}} - \chi_{\mathrm{p}}$. Intuitively, it should

depend on the cross-track error itself, such that$\chi_{\mathrm{r}} = \chi_{\mathrm{r}}(e)$. An attractive choice for $\chi_{\mathrm{r}}(e)$ could then be the physically motivated:

$$\chi_{\mathrm{r}}(e) = \arctan\left(-\frac{e}{\triangle_{\mathrm{e}}}\right), \tag{19}$$

where $\triangle_{\mathrm{e}}$ becomes a time-varying guidance variable satisfying A.3, utilized to shape the convergence behaviour towards the longitudinal axis of **P**. Such a variable is often referred to as a *lookahead distance* in literature dealing with planar path following along straight lines [9], and the physical interpretation can be derived from Figure 1. Note that other sigmoidal shaping functions are also possible candidates for $\chi_{\mathrm{r}}(e)$, for instance the $\tanh$ function. Consequently, the desired azimuth angle is given by:

$$\chi_{\mathrm{d}}(\varpi, e) = \chi_{\mathrm{p}}(\varpi) + \chi_{\mathrm{r}}(e), \tag{20}$$

with $\chi_{\mathrm{p}}(\varpi)$ as in (3) and $\chi_{\mathrm{r}}(e)$ as in (19).

Since ϖ is the actual path parametrization variable that we control for guidance purposes, we need to obtain a relationship between ϖ and U_{p} to be able to implement (17). By using the kinematic relationship given by (12), we get that:

$$\begin{aligned} \dot{\varpi} &= \frac{U_{\mathrm{p}}}{\sqrt{x_{\mathrm{p}}'^2 + y_{\mathrm{p}}'^2}} \\ &= \frac{U_{\mathrm{d}}\cos\chi_{\mathrm{r}} + \gamma s}{\sqrt{x_{\mathrm{p}}'^2 + y_{\mathrm{p}}'^2}}, \end{aligned} \tag{21}$$

which is non-singular for all paths satisfying assumption A.1. This also shows that **P** is not a so-called Serret-Frenet frame, which is defined at the exact projection point of the ideal particle onto the geometric path.

Consequently, by utilizing trigonometric relationships from Figure 1, the derivative of the CLF finally becomes:

$$\dot{V}_{\boldsymbol{\varepsilon}} = -\gamma s^2 - U_{\mathrm{d}}\frac{e^2}{\sqrt{e^2 + \triangle_{\mathrm{e}}^2}}, \tag{22}$$

which is negative definite under assumptions A.2 and A.3.

Elaborating on these results, we find that the total dynamic system, which consists of the ideal particle and the path particle, can be represented by the states $\boldsymbol{\varepsilon}$ and ϖ. Moreover, the dynamics are non-autonomous since U_{d} and $\triangle_{\mathrm{e}}$ can be time-varying. However, by reformulating the time dependence through the introduction of an extra state, the augmented system can be made autonomous:

$$\dot{l} = 1, \;\; l_0 = t_0 \geq 0, \tag{23}$$

see e.g. Teel et al. [10]. Hence, the augmented system can be represented by the state vector $\mathbf{x} = \left[\boldsymbol{\varepsilon}^\top, \varpi, l\right]^\top \in \mathbb{R}^2 \times \mathbb{R} \times \mathbb{R}_{\geq 0}$, and with dynamics represented by the time-invariant ordinary differential equation:

$$\dot{\mathbf{x}} = \mathbf{f}(\mathbf{x}). \tag{24}$$

The time variable for the augmented system is denoted t with initial time $t = 0$, such that $l(t) = t + t_0$. The motivation for this reformulation is that it allows us to utilize set stability analysis for time-invariant systems when concluding on whether the task objectives in the problem statement have been met or not. Hence, define the closed, but unbounded set:

$$\mathcal{E} = \left\{\mathbf{x} \in \mathbb{R}^2 \times \mathbb{R} \times \mathbb{R}_{\geq 0} \mid \boldsymbol{\varepsilon} = \mathbf{0}\right\}, \tag{25}$$

which represents the dynamics of the augmented system when the ideal particle has converged to the path particle, i.e. converged to the desired geometric path. Also, let:

$$\begin{aligned} |\mathbf{x}|_{\mathcal{E}} &= \inf\left\{\mathbf{x} - \mathbf{y} \mid \mathbf{y} \in \mathcal{E}\right\} && (26) \\ &= (\boldsymbol{\varepsilon}^\top \boldsymbol{\varepsilon})^{\frac{1}{2}} && (27) \end{aligned}$$

represent a function measuring the distance from $\mathbf{x}$ to $\mathcal{E}$, i.e. the off-track error. Making $|\mathbf{x}|_{\mathcal{E}}$ converge to zero is equivalent to solving the geometric task of the guidance-based path following problem, and the following proposition can now be stated:

Proposition 1: The error set $\mathcal{E}$ is rendered uniformly globally asymptotically and locally exponentially stable (UGAS/ULES) under assumptions A.1-A.3 if ϖ is updated by (21), and χ_{r} is equal to (19).

Proof: Since the set $\mathcal{E}$ is closed, but not bounded, we initially have to make sure that the dynamic system (24) is forward complete [10], i.e. that for each $\mathbf{x}_0$ the solution $\mathbf{x}(t, \mathbf{x}_0)$ is defined on $[0, \infty\rangle$. This entails that the solution cannot escape to infinity in finite time. By definition, l cannot escape in finite time. Also, (14) and (22) shows that neither can $\boldsymbol{\varepsilon}$. Consequently, (21) shows that ϖ cannot escape in finite time under assumptions A.1 and A.2. The system is therefore forward complete. We also know that $\forall \mathbf{x}_0 \in \mathcal{E}$ the solution $\mathbf{x}(t, \mathbf{x}_0) \in \mathcal{E}\ \forall t \geq 0$ because $\boldsymbol{\varepsilon}_0 = \mathbf{0} \Rightarrow \dot{\boldsymbol{\varepsilon}} = \mathbf{0}$. This renders $\mathcal{E}$ forward invariant for (24) since the system is already shown to be forward complete. Now, having established that (24) is forward complete and that $\mathcal{E}$ is forward invariant, and considering the fact that $V_{\boldsymbol{\varepsilon}} = \frac{1}{2}\boldsymbol{\varepsilon}^\top\boldsymbol{\varepsilon} = \frac{1}{2}(|\mathbf{x}|_{\mathcal{E}})^2$, we can derive our stability results by considering the properties of $V_{\boldsymbol{\varepsilon}}$, see e.g. [8]. Hence, we conclude by standard Lyapunov arguments that the error set $\mathcal{E}$ is rendered UGAS. Furthermore, $\dot{V}_{\boldsymbol{\varepsilon}} = -\gamma s^2 - \frac{U_{\mathrm{d}}}{\triangle_{\mathrm{e}}}e^2 \leq -\gamma s^2 - \frac{U_{\mathrm{d,min}}}{\triangle_{\mathrm{e,max}}}e^2$ for the error dynamics at $\boldsymbol{\varepsilon} = \mathbf{0}$, which proves ULES. ■

By stabilizing the error set $\mathcal{E}$, we have achieved the geometric task. The dynamic task is fulfilled by assigning a desired speed U_{d} which satisfies assumption A.2. In total, we have now solved the planar guidance-based path following problem.

Note that by choosing the speed of the ideal particle equal to:

$$U_{\mathrm{d}} = \kappa\sqrt{e^2 + \triangle_{\mathrm{e}}^2}, \tag{28}$$

where $\kappa > 0$ is a constant gain parameter, we obtain:

$$\dot{V}_{\boldsymbol{\varepsilon}} = -\gamma s^2 - \kappa e^2, \tag{29}$$

which results in the following proposition:

Proposition 2: The error set $\mathcal{E}$ is rendered uniformly globally exponentially stable (UGES) under assumptions A.1 and A.3 if ϖ is updated by (21), χ_{r} is equal to (19), and U_{d} satisfies (28).

Proof: The first part of the proof is identical to that of Proposition 1. Hence, we conclude by standard Lyapunov arguments that the error set $\mathcal{E}$ is rendered UGES. ■

Although very powerful, this result is clearly not achievable by physical systems since these exhibit natural limitations on their maximum attainable speed. In this regard, Proposition 1 states the best possible stability property a planar physical system like a watercraft can hold.

C. Principles of Guidance in 3D

This section treats the spatial 3D case of the guidance-based path following problem, and the procedure for obtaining the guidance laws is essentially the same as for the planar 2D case.

Denote the inertial position and velocity vectors of the ideal particle by $\mathbf{p} = [x, y, z]^\top \in \mathbb{R}^3$ and $\dot{\mathbf{p}} = [\dot{x}, \dot{y}, \dot{z}]^\top \in \mathbb{R}^3$, respectively. Denote the size of the velocity vector by $U = |\dot{\mathbf{p}}|_2 = (\dot{\mathbf{p}}^\top \dot{\mathbf{p}})^{\frac{1}{2}}$ (the speed), and let the orientation be characterized by the two angular variables:

$$\chi = \arctan\left(\frac{\dot{y}}{\dot{x}}\right), \tag{30}$$

which is denoted the azimuth angle, and:

$$\upsilon = \arctan\left(\frac{-\dot{z}}{\sqrt{\dot{x}^2 + \dot{y}^2}}\right), \tag{31}$$

denoted the elevation angle. Since it is assumed that for an ideal particle U, χ and υ can attain any desirable value instantaneously, rewrite them as U_{d}, χ_{d} and υ_{d}.

Consider a geometric path continuously parametrized by a scalar variable $\varpi \in \mathbb{R}$, and denote the position of its path particle as $\mathbf{p}_{\mathrm{p}}(\varpi) \in \mathbb{R}^3$. Consequently, the geometric path can be expressed by the set:

$$\mathcal{P} = \left\{\mathbf{p} \in \mathbb{R}^3 \mid \mathbf{p} = \mathbf{p}_{\mathrm{p}}(\varpi)\ \forall \varpi \in \mathbb{R}\right\}, \tag{32}$$

where $\mathcal{P} \subset \mathbb{R}^3$.

For a given ϖ, define a local reference frame at $\mathbf{p}_{\mathrm{p}}(\varpi)$ and name it the PATH frame (**P**). To arrive at **P**, we need to perform two consecutive elementary rotations (when using the concept of Euler angles). The first is to positively rotate the INERTIAL frame (**I**) an angle:

$$\chi_{\mathrm{p}}(\varpi) = \arctan\left(\frac{y'_{\mathrm{p}}(\varpi)}{x'_{\mathrm{p}}(\varpi)}\right) \tag{33}$$

about its z-axis. This rotation can be represented by the rotation matrix:

$$\mathbf{R}_{\mathrm{p,z}}(\chi_{\mathrm{p}}) = \begin{bmatrix} \cos\chi_{\mathrm{p}} & -\sin\chi_{\mathrm{p}} & 0 \\ \sin\chi_{\mathrm{p}} & \cos\chi_{\mathrm{p}} & 0 \\ 0 & 0 & 1 \end{bmatrix}, \tag{34}$$

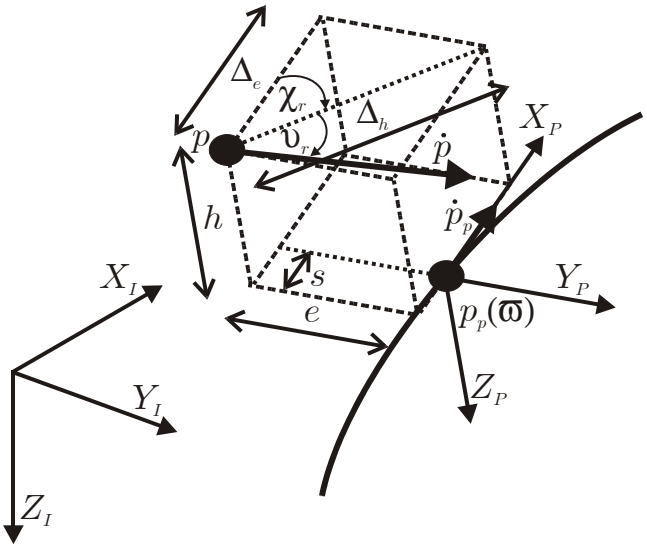

Fig. 2. The geometric relationship between all the relevant parameters and variables utilized in the proposed guidance-based path following scheme in 3D, $\mu = 1$.

where $\mathbf{R}_{\mathrm{p,z}} \in SO(3)$. The second rotation is performed by positively rotating the resulting intermediate frame an angle:

$$\upsilon_{\mathrm{p}}(\varpi) = \arctan\left(\frac{-z'_{\mathrm{p}}(\varpi)}{\sqrt{x'_{\mathrm{p}}(\varpi)^2 + y'_{\mathrm{p}}(\varpi)^2}}\right) \tag{35}$$

about its y-axis. This rotation can be represented by the rotation matrix:

$$\mathbf{R}_{\mathrm{p,y}}(\upsilon_{\mathrm{p}}) = \begin{bmatrix} \cos\upsilon_{\mathrm{p}} & 0 & \sin\upsilon_{\mathrm{p}} \\ 0 & 1 & 0 \\ -\sin\upsilon_{\mathrm{p}} & 0 & \cos\upsilon_{\mathrm{p}} \end{bmatrix}, \tag{36}$$

where $\mathbf{R}_{\mathrm{p,y}} \in SO(3)$. Hence, the full rotation can be represented by the rotation matrix:

$$\mathbf{R}_{\mathrm{p}} = \mathbf{R}_{\mathrm{p,z}}(\chi_{\mathrm{p}})\mathbf{R}_{\mathrm{p,y}}(\upsilon_{\mathrm{p}}), \tag{37}$$

where $\mathbf{R}_{\mathrm{p}} \in SO(3)$. Consequently, the error vector between $\mathbf{p}$ and $\mathbf{p}_{\mathrm{p}}(\varpi)$ expressed in **P** is given by:

$$\boldsymbol{\varepsilon} = \mathbf{R}_{\mathrm{p}}^\top(\mathbf{p} - \mathbf{p}_{\mathrm{p}}(\varpi)), \tag{38}$$

where $\boldsymbol{\varepsilon} = [s, e, h]^\top \in \mathbb{R}^3$ consists of the *along-track error* s, the *cross-track error* e, and the *vertical-track error* h; see Figure 2. The along-track error represents the distance from $\mathbf{p}_{\mathrm{p}}(\varpi)$ to $\mathbf{p}$ along the x-axis of the PATH frame, the cross-track error represents the distance along the y-axis, while the vertical-track error represents the distance along the z-axis. Also, recognize the notions of the *horizontal-track error* $\sqrt{s^2 + e^2}$, the *generalized cross-track error* $\sqrt{e^2 + h^2}$, and the *off-track error* $\sqrt{s^2 + e^2 + h^2}$.

The error set in question is now given by:

$$\mathcal{E} = \left\{\mathbf{x} \in \mathbb{R}^3 \times \mathbb{R} \times \mathbb{R}_{\geq 0} \mid \boldsymbol{\varepsilon} = \mathbf{0}\right\}, \tag{39}$$

with the associated distance function:

$$|\mathbf{x}|_{\mathcal{E}} = \inf\{\mathbf{x}-\mathbf{y} \mid \mathbf{y}\in\mathcal{E}\} \quad (40)$$
$$= (\boldsymbol{\varepsilon}^\top\boldsymbol{\varepsilon})^{\frac{1}{2}}, \quad (41)$$

i.e. the off-track error. As in the 2D case, making $|\mathbf{x}|_{\mathcal{E}}$ converge to zero is equivalent to solving the geometric task of the guidance-based path following problem.

By differentiating $\boldsymbol{\varepsilon}$ with respect to time, we obtain:

$$\dot{\boldsymbol{\varepsilon}} = \dot{\mathbf{R}}_{\mathrm{p}}^\top(\mathbf{p}-\mathbf{p}_{\mathrm{p}}) + \mathbf{R}_{\mathrm{p}}^\top(\dot{\mathbf{p}}-\dot{\mathbf{p}}_{\mathrm{p}}), \quad (42)$$

where:

$$\dot{\mathbf{R}}_{\mathrm{p}} = \mathbf{R}_{\mathrm{p}}\mathbf{S}_{\mathrm{p}} \quad (43)$$

with:

$$\mathbf{S}_{\mathrm{p}} = \begin{bmatrix} 0 & -\dot{\chi}_{\mathrm{p}}\cos\upsilon_{\mathrm{p}} & \dot{\upsilon}_{\mathrm{p}} \\ \dot{\chi}_{\mathrm{p}}\cos\upsilon_{\mathrm{p}} & 0 & \dot{\chi}_{\mathrm{p}}\sin\upsilon_{\mathrm{p}} \\ -\dot{\upsilon}_{\mathrm{p}} & -\dot{\chi}_{\mathrm{p}}\sin\upsilon_{\mathrm{p}} & 0 \end{bmatrix}, \quad (44)$$

which is skew-symmetric; $\mathbf{S}_{\mathrm{p}} = -\mathbf{S}_{\mathrm{p}}^\top$. We also have that:

$$\dot{\mathbf{p}} = \dot{\mathbf{p}}_{\mathrm{dv}} = \mathbf{R}_{\mathrm{dv}}\mathbf{v}_{\mathrm{dv}}, \quad (45)$$

where $\mathbf{R}_{\mathrm{dv}} \in SO(3)$ represents a rotation matrix from the INERTIAL frame to a frame attached to the ideal particle with its x-axis along the velocity vector of the particle. Let this frame be called the DESIRED VELOCITY frame (**DV**). Hence, the vector $\mathbf{v}_{\mathrm{dv}} = [U_{\mathrm{d}}, 0, 0]^\top \in \mathbb{R}^3$ represents the ideal particle velocity with respect to **I**, represented in **DV**. Then inspired by the approach in the 2D case, the rotation matrix $\mathbf{R}_{\mathrm{dv}}$ is directly selected to be defined by:

$$\mathbf{R}_{\mathrm{dv}} = \mathbf{R}_{\mathrm{p}}\mathbf{R}_{\mathrm{r}}, \quad (46)$$

where:

$$\mathbf{R}_{\mathrm{r}} = \mathbf{R}_{\mathrm{r,z}}(\chi_{\mathrm{r}})\mathbf{R}_{\mathrm{r,y}}(\upsilon_{\mathrm{r}}) \quad (47)$$

with $\mathbf{R}_{\mathrm{r}}$, $\mathbf{R}_{\mathrm{r,z}}$, and $\mathbf{R}_{\mathrm{r,y}}$ all elements of $SO(3)$. This way of defining $\mathbf{R}_{\mathrm{dv}}$ entails that the **DV** frame is obtained by first performing an initial rotation represented by $\mathbf{R}_{\mathrm{p}}$, resulting in an intermediate frame parallel to the **P** frame, before a relative rotation represented by $\mathbf{R}_{\mathrm{r}}$ is performed to arrive in **DV**. Consequently, $\mathbf{R}_{\mathrm{r}}$ (i.e. the angular variables χ_{r} and υ_{r}) must be designed to ensure that the generalized cross-track error approaches zero (while $\mathbf{R}_{\mathrm{r}}$ approaches **I**).

Continuing to elaborate on (42), we also have that:

$$\dot{\mathbf{p}}_{\mathrm{p}} = \mathbf{R}_{\mathrm{p}}\mathbf{v}_{\mathrm{p}}, \quad (48)$$

where $\mathbf{v}_{\mathrm{p}} = [U_{\mathrm{p}}, 0, 0]^\top \in \mathbb{R}^3$ represents the path particle velocity with respect to **I**, represented in **P**.

By then expanding (42) in light of the recent discussion, we get:

$$\dot{\boldsymbol{\varepsilon}} = (\mathbf{R}_{\mathrm{p}}\mathbf{S}_{\mathrm{p}})^\top(\mathbf{p}-\mathbf{p}_{\mathrm{p}}) + \mathbf{R}_{\mathrm{p}}^\top(\mathbf{R}_{\mathrm{dv}}\mathbf{v}_{\mathrm{dv}} - \mathbf{R}_{\mathrm{p}}\mathbf{v}_{\mathrm{p}})$$
$$= \mathbf{S}_{\mathrm{p}}^\top\boldsymbol{\varepsilon} + \mathbf{R}_{\mathrm{r}}\mathbf{v}_{\mathrm{dv}} - \mathbf{v}_{\mathrm{p}}. \quad (49)$$

Now define the positive definite and radially unbounded Control Lyapunov Function (CLF):

$$V_{\boldsymbol{\varepsilon}} = \frac{1}{2}\boldsymbol{\varepsilon}^\top\boldsymbol{\varepsilon} = \frac{1}{2}(s^2+e^2+h^2), \quad (50)$$

and differentiate it with respect to time along the trajectories of $\boldsymbol{\varepsilon}$ to obtain:

$$\dot{V}_{\boldsymbol{\varepsilon}} = \boldsymbol{\varepsilon}^\top\dot{\boldsymbol{\varepsilon}}$$
$$= \boldsymbol{\varepsilon}^\top\left(\mathbf{S}_{\mathrm{p}}^\top\boldsymbol{\varepsilon} + \mathbf{R}_{\mathrm{r}}\mathbf{v}_{\mathrm{dv}} - \mathbf{v}_{\mathrm{p}}\right)$$
$$= \boldsymbol{\varepsilon}^\top\left(\mathbf{R}_{\mathrm{r}}\mathbf{v}_{\mathrm{dv}} - \mathbf{v}_{\mathrm{p}}\right) \quad (51)$$

since the skew-symmetry of $\mathbf{S}_{\mathrm{p}}$ leads to $\boldsymbol{\varepsilon}^\top\mathbf{S}_{\mathrm{p}}^\top\boldsymbol{\varepsilon} = 0$. By further expansion, we get:

$$\dot{V}_{\boldsymbol{\varepsilon}} = s(U_{\mathrm{d}}\cos\chi_{\mathrm{r}}\cos\upsilon_{\mathrm{r}} - U_{\mathrm{p}}) + eU_{\mathrm{d}}\sin\chi_{\mathrm{r}}\cos\upsilon_{\mathrm{r}} - hU_{\mathrm{d}}\sin\upsilon_{\mathrm{r}}, \quad (52)$$

from where we choose U_{p} as:

$$U_{\mathrm{p}} = U_{\mathrm{d}}\cos\chi_{\mathrm{r}}\cos\upsilon_{\mathrm{r}} + \gamma s, \quad (53)$$

where $\gamma > 0$ becomes a constant gain parameter in the guidance law. Since ϖ is the actual path parametrization variable that we control for guidance purposes, we need to obtain a relationship between ϖ and U_{p} to be able to implement (53). By using the kinematic relationship given by (48), we get that:

$$\dot{\varpi} = \frac{U_{\mathrm{d}}\cos\chi_{\mathrm{r}}\cos\upsilon_{\mathrm{r}} + \gamma s}{\sqrt{x_{\mathrm{p}}'^2 + y_{\mathrm{p}}'^2 + z_{\mathrm{p}}'^2}}, \quad (54)$$

which is non-singular for all paths satisfying assumption A.1. By choosing U_{p} this way, we achieve:

$$\dot{V}_{\boldsymbol{\varepsilon}} = -\gamma s^2 + eU_{\mathrm{d}}\sin\chi_{\mathrm{r}}\cos\upsilon_{\mathrm{r}} - hU_{\mathrm{d}}\sin\upsilon_{\mathrm{r}}. \quad (55)$$

As in the 2D case, an attractive choice for χ_{r} could be the physically motivated:

$$\chi_{\mathrm{r}}(e) = \arctan\left(-\frac{e}{\triangle_{\mathrm{e}}}\right), \quad (56)$$

where $\triangle_{\mathrm{e}}$ becomes a time-varying guidance variable satisfying A.3, utilized to shape the convergence behaviour towards the xz-plane of **P**.

The choice for υ_{r} could then be:

$$\upsilon_{\mathrm{r}}(h) = \arctan\left(\frac{h}{\triangle_{\mathrm{h}}}\right), \quad (57)$$

where $\triangle_{\mathrm{h}}$ becomes an additional time-varying guidance variable satisfying A.3. It is utilized to shape the convergence behaviour towards the xy-plane of **P**. Consequently, by using trigonometric relationships from Figure 2, the derivative of the CLF finally becomes:

$$\dot{V}_{\boldsymbol{\varepsilon}} = -\gamma s^2 - U_{\mathrm{d}}\left[\cos\upsilon_{\mathrm{r}}\frac{e^2}{\sqrt{e^2+\triangle_{\mathrm{e}}^2}} + \frac{h^2}{\sqrt{h^2+\triangle_{\mathrm{h}}^2}}\right], \quad (58)$$

which is negative definite under assumptions A.2 and A.3. The following proposition can now be stated:

Proposition 3: The error set $\mathcal{E}$ is rendered uniformly globally asymptotically and locally exponentially stable (UGAS/ULES) under assumptions A.1-A.3 if ϖ is updated by (54), χ_{r} is equal to (56), and υ_{r} is equal to (57).

Proof: The first part of the proof is identical to that of Proposition 1. Hence, we conclude by standard Lyapunov arguments that the error set $\mathcal{E}$ is rendered UGAS. Furthermore, $\dot{V}_{\boldsymbol{\varepsilon}} = -\gamma s^2 - U_{\mathrm{d}} \left[\frac{e^2}{\triangle_{\mathrm{e}}} + \frac{h^2}{\triangle_{\mathrm{h}}} \right] \leq -\gamma s^2 - U_{\mathrm{d,min}} \left[\frac{e^2}{\triangle_{\mathrm{e,max}}} + \frac{h^2}{\triangle_{\mathrm{h,max}}} \right]$ for the error dynamics at $\boldsymbol{\varepsilon} = \mathbf{0}$, which proves ULES. ■

By stabilizing the error set $\mathcal{E}$, we have achieved the geometric task. The dynamic task is fulfilled by assigning a desired speed U_{d} which satisfies assumption A.2. In total, we have now solved the spatial guidance-based path following problem.

Since $\triangle_{\mathrm{h}}$ can be expressed as:

$$\triangle_{\mathrm{h}} = \mu \sqrt{e^2 + \triangle_{\mathrm{e}}^2}, \tag{59}$$

where $\mu > 0$, we can rewrite (58) as:

$$\dot{V}_{\boldsymbol{\varepsilon}} = -\gamma s^2 - U_{\mathrm{d}} \left[\frac{\mu e^2 + h^2}{\sqrt{\mu^2 (e^2 + \triangle_{\mathrm{e}}^2) + h^2}} \right] \tag{60}$$

because:

$$\cos \upsilon_{\mathrm{r}} = \frac{\mu \sqrt{e^2 + \triangle_{\mathrm{e}}^2}}{\sqrt{\mu^2 (e^2 + \triangle_{\mathrm{e}}^2) + h^2}} \tag{61}$$

when expressing $\triangle_{\mathrm{h}}$ as in (59). By choosing the desired speed of the ideal particle as:

$$U_{\mathrm{d}} = \kappa \sqrt{\mu^2 (e^2 + \triangle_{\mathrm{e}}^2) + h^2}, \tag{62}$$

where $\kappa > 0$ is a constant gain parameter, we obtain:

$$\dot{V}_{\boldsymbol{\varepsilon}} = -\gamma s^2 - \mu \kappa e^2 - \kappa h^2, \tag{63}$$

which results in the following proposition:

Proposition 4: The error set $\mathcal{E}$ is rendered uniformly globally exponentially stable (UGES) under assumptions A.1 and A.3 if ϖ is updated by (54), χ_{r} is equal to (56), υ_{r} is equal to (57), and U_{d} satisfies (62).

Proof: The first part of the proof is identical to that of Proposition 1. Hence, we conclude by standard Lyapunov arguments that the error set $\mathcal{E}$ is rendered UGES. ■

As mentioned in the 2D case, the prerequisite for this result is not practically achievable by physical systems. Hence, Proposition 3 states the best possible stability property a spatial physical system like a spacecraft can hold.

After having obtained the guidance laws of this section by defining and elaborating on an $\mathbf{R}_{\mathrm{dv}}$ which is constructed by four elementary rotations, and partially defined by $\mathbf{R}_{\mathrm{p}}$, we would now like to define an $\mathbf{R}_{\mathrm{dv}}$ which is constructed by only two elementary rotations. This is interesting from a control perspective, especially if we choose not to operate directly in the configuration space. Hence, consider an $\mathbf{R}_{\mathrm{dv}}$ defined by a positive rotation about the z-axis of $\mathbf{I}$ by a desired azimuth angle χ_{d}, followed by a positive rotation about the y-axis of the resulting intermediate frame by a desired elevation angle υ_{d}:

$$\mathbf{R}_{\mathrm{dv}} = \mathbf{R}_{\mathrm{dv,z}}(\chi_{\mathrm{d}}) \mathbf{R}_{\mathrm{dv,y}}(\upsilon_{\mathrm{d}}), \tag{64}$$

Fig. 3. Examples of mechanical systems operating in 2D or 3D, ranging from watercraft and landcraft to aircraft and spacecraft.

where $\mathbf{R}_{\mathrm{dv,z}}$ and $\mathbf{R}_{\mathrm{dv,y}}$ both are elements of $SO(3)$. Obviously, the rotations represented by (46) and (64) are not equivalent, i.e. the y- and z-axes of the two resulting frames are not aligned. However, the rotations map the velocity vector $\mathbf{v}_{\mathrm{dv}}$ equivalently to the INERTIAL frame, which is what matters here. Therefore, by equating the first column (which represents a rotation of the x-axis) of (46) with that of (64), we obtain:

$$\chi_{\mathrm{d}} = \arctan \left(\begin{array}{c} \frac{\cos \chi_{\mathrm{p}} \sin \chi_{\mathrm{r}} \cos \upsilon_{\mathrm{r}} + \cdots}{- \sin \chi_{\mathrm{p}} \sin \chi_{\mathrm{r}} \cos \upsilon_{\mathrm{r}} + \cdots} \\ \frac{- \sin \upsilon_{\mathrm{p}} \sin \upsilon_{\mathrm{r}} \sin \chi_{\mathrm{p}} + \cdots}{- \sin \upsilon_{\mathrm{p}} \sin \upsilon_{\mathrm{r}} \cos \chi_{\mathrm{p}} + \cdots} \\ \frac{\sin \chi_{\mathrm{p}} \cos \chi_{\mathrm{r}} \cos \upsilon_{\mathrm{p}} \cos \upsilon_{\mathrm{r}}}{\cos \chi_{\mathrm{p}} \cos \chi_{\mathrm{r}} \cos \upsilon_{\mathrm{p}} \cos \upsilon_{\mathrm{r}}} \end{array} \right), \tag{65}$$

and

$$\upsilon_{\mathrm{d}} = \arcsin(\sin \upsilon_{\mathrm{p}} \cos \upsilon_{\mathrm{r}} \cos \chi_{\mathrm{r}} + \cos \upsilon_{\mathrm{p}} \sin \upsilon_{\mathrm{r}}), \tag{66}$$

which are the angular variables that the velocity vector orientation of the ideal particle must adhere to in order to ensure geometric path convergence. Note that through the use of trigonometric addition formulas, it can be shown that (65) is equivalent to (20) in the 2D case, i.e. when $\upsilon_{\mathrm{p}} = \upsilon_{\mathrm{r}} = 0$.

IV. Possible Applications and Extensions to the Guidance-Based Path Following Concept

The concept of guidance-based path following could certainly be directly applied to achieve natural motion behaviour of moving objects in fields like computer animation and computer games in an easy and intuitive way. But more importantly, it could also be applied to the motion control of mechanical systems operating in a 2D plane or a 3D space like for instance watercraft or spacecraft, see e.g. Figure 3. The extension to such physical target systems could be achieved by tailoring the guidance concepts on a case-by-case basis, considering carefully the specifics pertaining to

each case, like for instance whether the system is fully actuated or underactuated. The resulting system could then be analysed by e.g. dynamic systems theory pertaining to cascades, see e.g. Loria [11]. In this regard, Figure 4 illustrates how the error dynamics of a closed loop dynamic system (e.g. like a controlled aircraft) would affect the guided ideal system considered in this paper through a cascaded interconnection.

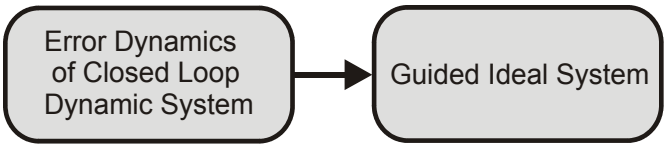

Fig. 4. The cascaded interconnection between the guided ideal system and the error dynamics of a closed loop dynamic system.

An interesting application of the guidance-based path following concept can already be found in [12]. The paper addresses the problem of creating a controller structure for the automatic control of a marine surface vessel through its entire speed regime without resorting to heuristics and switching between structurally different controllers, as is usually the case. Hence, a single controller structure is proposed for the purpose. Its core is a nonlinear, model-based velocity and heading controller which relies on the guidance-based path following concept to ensure geometric path convergence. All regular paths are rendered feasible, and the scheme ensures that a vessel which is fully actuated at low speeds, but becomes underactuated at high speeds, is able to converge to and follow a desired geometric path independent of the actual vessel speed.

It is expected that the guidance-base path following approach will render possible a more natural and energy efficient motion behaviour of mechanical vehicle systems than what is currently the case when applying for instance a traditional trajectory tracking approach. This relates to the fact that the alteration of the employed guidance parameters and variables directly and intuitively affects the transient path convergence behaviour, and consequently can be applied to shape it as desired. Such a feature is also desirable for more abstract n-dimensional systems, to which the concept is readily extendable.

The main purpose of any guidance system is to compute all the reference signals that are necessary to render a given physical system autonomous under feedback control. In this context, the guidance laws proposed in this paper represent only what lies at the core of a guidance system, which fully equipped consists of a plethora of algorithms providing advanced features like obstacle avoidance, formation control and synchronization capabilities. Consequently, it is of great interest to extend the present guidance framework towards such advanced guidance concepts.

V. Conclusions

This paper has treated the subject of fundamental guidance principles related to motion behaviour in a 2D plane and a 3D space. The concept of guidance-based path following has been defined and elaborated upon, and its specifics contrasted towards the already established concept of trajectory tracking. Guidance laws have been developed at an ideal, dynamics-independent level to prevent any obfuscation by particularities stemming from any specific dynamics case. The result is generally valid laws which can be tailored to specific target systems like e.g. watercraft or spacecraft, for instance in a cascaded setting. The scheme renders all regular paths feasible. Furthermore, it is possible that the approach can lead to a more natural convergence behaviour of certain mechanical vehicle systems towards desired geometric paths than what is currently achieved by applying a traditional trajectory tracking approach. Finally, possible applications and extensions to the guidance-based path following scheme have been briefly suggested.

References

[1] C. Samson, “Path following and time-varying feedback stabilization of a wheeled mobile robot,” in *Proceedings of the ICARCV’92, Singapore*, 1992.

[2] R. Rysdyk, “UAV path following for constant line-of-sight,” in *Proceedings of the 2nd AIAA "Unmanned Unlimited" Systems, Technologies, and Operations - Aerospace, San Diego, California, USA*, 2003.

[3] K. Y. Pettersen and E. Lefeber, “Way-point tracking control of ships,” in *Proceedings of the 40th IEEE CDC, Orlando, Florida, USA*, 2001.

[4] L. Lapierre, D. Soetanto, and A. Pascoal, “Nonlinear path following with applications to the control of autonomous underwater vehicles,” in *Proceedings of the 42nd IEEE CDC, Maui, Hawaii, USA*, 2003.

[5] K. D. Do and J. Pan, “Robust path following of underactuated ships using serret-frenet frame,” in *Proceedings of the ACC’03, Denver, Colorado, USA*, 2003.

[6] P. Encarnação and A. Pascoal, “3D path following for autonomous underwater vehicles,” in *Proceedings of the 39th IEEE CDC, Sydney, Australia*, 2000.

[7] F. D. del Río, G. Jiménez, J. L. Sevillano, S. Vicente, and A. C. Balcells, “A generalization of path following for mobile robots,” in *Proceedings of the ICRA’99, Detroit, Michigan, USA*, 1999.

[8] R. Skjetne, “The maneuvering problem,” Ph.D. dissertation, Norwegian University of Science and Technology, Trondheim, Norway, 2005.

[9] F. A. Papoulias, “Bifurcation analysis of line of sight vehicle guidance using sliding modes,” *International Journal of Bifurcation and Chaos*, vol. 1, no. 4, pp. 849–865, 1991.

[10] A. Teel, E. Panteley, and A. Loría, “Integral characterization of uniform asymptotic and exponential stability with applications,” *Mathematics of Control, Signals, and Systems*, vol. 15, pp. 177–201, 2002.

[11] A. Loría, “Cascaded nonlinear time-varying systems: Analysis and design,” 2004, lecture notes, Minicourse at ECTS, France.

[12] M. Breivik and T. I. Fossen, “A unified concept for controlling a marine surface vessel through the entire speed envelope,” in *Proceedings of the MED’05, Limassol, Cyprus*, 2005.